Proceedings of the 21st National & 10th ISHMT-ASME Heat and Mass Transfer Conference

December 27-30, 2011, IIT Madras, India

ISHMT_IND_02_041

ESTIMATION OF LAMINAR SINGLE-PHASE HEAT TRANSFER COEFFICIENT IN THE ENTRANCE REGION OF A SQUARE MINICHANNEL USING INFRA-RED THERMOGRAPHY

Balkrishna Mehta
Department of Mechanical Engineering
Indian Institute of Technology Kanpur
Kanpur 208016 India

Abhimanyu Dhyani
Department of Mechanical Engineering
Indian Institute of Technology Kanpur
Kanpur 208016 India

Sameer Khandekar*
Department of Mechanical Engineering
Indian Institute of Technology Kanpur
Kanpur 208016 India
samkhan@iitk.ac.in

(* Corresponding Author)

ABSTRACT

Inherently high heat transfer coefficients during single-phase developing laminar flow regions are of interest in mini/micro systems. Experimental determination of these high transfer coefficients is challenging. We report estimation of local Nu for hydrodynamically fully developed but thermally developing single-phase laminar flow of water, in a square mini-channel (aluminum test section of square cross section 5 mm x 5 mm x 140 mm) using non-intrusive Infra-Red Thermography (IRT). Constant heat flux condition is applied at the bottom of the substrate, top face being adiabatic. Flow Re varies from 330-850. IRT is used to measure the wall temperature and the local heat flux at the channel wall-fluid interface is approximated by assuming 1-D conduction in the transverse direction. A 3D-CFD model, following the exact geometry and boundary conditions of the experimental setup, is also developed and results are compared. It is observed that although the setup is prone to conjugate effects resulting in axial back conduction in the substrate, this does not affect the estimation of local Nusselt number significantly.

Keywords: *mini-channel, thermally developing flow, Infra-Red thermography, conjugate effects.*

INTRODUCTION

High heat flux removal from confined geometries is a contemporary problem. Turbulence creation is difficult at such small scales and therefore heat transport enhancement techniques in the laminar region need to be understood and implemented. Experimental determination of transfer coefficients in mini/micro geometries is difficult because (a) the ratio of area of cross sections for the heat flow in the solid substrate to that of the fluid domain is usually either comparable or can even be quite large. Due to this, the heat transfer boundary condition which the fluid actually experiences at the solid-fluid interface significantly deviates from the conventional UHF (Uniform Heat Flux) or UWT (Uniform Wall Temperature), as is conceived mathematically, (b) Intrusive point measurements, for example thermometry and velocimetry, also defeat the purpose as they disrupt the thermal and hydrodynamic flow behavior, and (c) Localized 3-D effects are more pronounced in the small scale systems leading to errors in averaging transport parameters. These limitations necessitate that the metrology of such systems be, as far as possible, non-intrusive and preferably should provide multi-dimensional, spatio-temporal information of the process parameters.

Infra-Red Thermography (IRT) is a rapidly developing technique for spatio-temporal thermal measurements (for example, see Hetsroni et al. [2003, 2011]; Sargent et al. [1998]; Astarita et al. [2003] and Kakuta et al. [2009]). As compared to other non-intrusive techniques like Liquid Crystal Thermography (LCT), it is much more versatile, repeatable and relatively easier to implement. In this work we employ IRT for the estimation of heat transfer in hydrodynamically fully developed but thermally developing laminar flows in mini-channel of size 5.0 mm x 5.0 mm. The design of the setup is such that the channel is part of an extended surface fin system, thus making the heat transfer conjugate in nature (See Figure 1 and detailed description in the next section). It should be noted that most practical engineering systems, especially on mini-micro scales, manifest conjugate heat transfer scenarios. As the heater source is located away from the channel, the thermal boundary condition at the fluid-wall interface is not identified as the conventional UHF or UWT. To establish this methodology for correct estimation of local heat transfer coefficient, the conjugate effects need to be discerned and the design of the setup should be such that effects of axial conduction on the estimation of local heat transfer are minimized, or at best quantifiable [for details refer, Luikov [1974]; Wang and Peng [1994]; Maranzana et al. [2004]; Gamrat et al. [2005]; Lee and Garimella [2006]; Celata et al. [2006]; Rao and Khandekar [2009]; Zhang et al. [2010] and Moharana et al. [2011]). In this work therefore, the baseline measurements are bench-marked against available analytical solutions. Moreover, CFD simulations are also carried out on a commercial platform for parametric studies which gives important insight into further improvement of the experimental setup.

EXPERIMENTAL SETUP/ PROCEDURE

The primary idea of the experimental design is to create an extended surface fin structure, one end of which is subjected to a constant heat flux boundary condition and the other end is subjected to a convective heat transfer boundary condition. The goal is to reduce the effect of axial conduction through the solid fin substrate in the streamwise direction and simultaneously to reduce the effective Biot number in the transverse direction at the channel wall, so as to get a good estimate of the local heat transfer coefficient.

The experimental facility, to meet the above requirements, is shown in Fig. 1(a). The test section consisted of single square mini-channel (5 mm x 5 mm x 140 mm; D_h = 5 mm), machined on an aluminum substrate (11 mm x 45 mm x 140 mm; k = 180 W/mK). The top of the channel was covered by a polycarbonate sheet (5.0 mm thick, k = 0.22 W/m-K), providing necessary insulation from top of the test section, as shown in the figure.

For providing constant heat flux boundary condition at one end of the aluminum substrate, a cylindrical DC supplied cartridge heater (diameter: 15 mm, length: 140 mm) was inserted, with the application of high conducting thermal paste (metal oxide filled silicon oil paste, RS components®, k = 2.9 W/mK). Digital multi-meters (accuracy ± 0.1 V and ±0.01 A) were used to measure the electrical power dissipation of the heater. The Biot number in the transverse direction was at least 5e-4, justifying the use of surface temperature from IRT for the wall temperature at the fluid-solid interface.

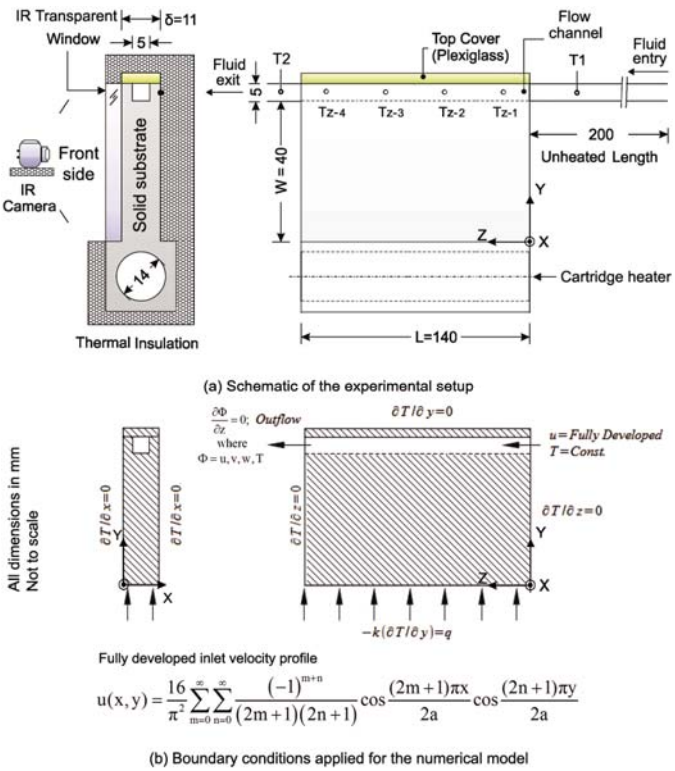

Figure 1: (a) Schematic of the experimental setup and, (b) boundary conditions for the CFD model.

The working fluid (distilled, degassed and deionized water) at a fixed temperature and mass flow rate, maintained by a constant temperature bath (Make: Julabo® F34 ME, accuracy ± 0.1 K), was made to pass through the mini-channel. The fluid temperatures at inlet and outlet of the test section respectively, were measured by suitably located K-type thermocouples (Omega®, 0.5 mm bead diameter, accuracy ±0.1 after calibration). All the surfaces of fin-substrate were completely insulated except an area of 25 mm x 130 mm at front surface which was covered by an Infra-red transmitting CaF_2 glass window (Make: Crystran®; Transmissivity: 95%, for wavelength 2 µm-7 µm, 5 mm thick; Refractive index = 1.39908 at 5 µm; k = 9.71 $Wm^{-1}K^{-1}$) to facilitate the recording of spatial IR thermographic profiles of the front surface of the fin-substrate. For bench-marking the camera and to measure the channel wall temperature at the back surface (behind the surface on which IR transparent glass was fitted; see Figure 1-a), four more K-type thermocouples were attached along the channel length (in the flow direction) at 10 mm, 50 mm, 90 mm and 130 mm from the channel inlet, as shown in Fig. 1(a). Thermocouple data acquisition was carried out at 1 Hz by using a high precision 12 bit PCI-DAQ card (Make: National Instruments®, PCI-6024E/ TBX-68 connector block). The IR camera used (Make: FLIR SC4000: Indium Antimonide detector array) had an operational spectral band of 3-5 µm, 14 bit signal digitization and a Noise Equivalent Temperature Difference of less than 0.02 K at 30°C. IR images were acquired and post processed by using ThermaCAM™ Researcher-V2.9 software.

- Emissivity correction:

For the correct measurement of surface temperature using IRT, the emissivity should be known accurately. During calibration (and subsequent experiments) temperatures were measured simultaneously by thermocouples and IR Camera. As Biot number in the X-direction is very small ~0.01, temperature gradients in this direction are negligible. When processing the IR image, tuning of emissivity was done to match the thermocouple readings at corresponding locations.

The difference between the electrical energy supplied to the channel and that received by the working fluid after steady state operation was measured and found to be always less than ~ 7-13 %, depending on the heat input. The Prandtl number of the fluid (= 5.5) is based on the fluid temperature at the channel inlet.

NUMERICAL SIMULATION

All CFD simulations were carried out using commercially software, Ansys-Fluent®6.3.26. A 3D model representing the exact dimensions of the experimental setup (one half of the setup was modeled at the available plane of symmetry) was constructed with GAMBIT-V-2.3.1®. The species conservation equations, along with the boundary conditions shown in Fig. 1-b, were solved. Typical grid sizes, after the grid independence were chosen to 25x25x140 for fluid domain and 25x90x140 for solid domain. Finer meshes were used near to the solid-fluid interface to resolve the gradients properly. 'SIMPLE' algorithm was employed for the pressure-velocity coupling. For descretization of momentum and energy equation, 'second order upwind' scheme has been applied. Interpolation of pressure is done by the 'Standard' scheme. For applying the fully developed inlet velocity profile condition, a user defined function was written. Absolute convergence criterion set for momentum was 10^{-6} and for that for the energy was 10^{-8}.

RESULTS AND DISCUSSION

The peripheral average local Nusselt number (Nu_z) for the square duct employed in the present study is defined as:

$$Nu_z = h_z \cdot D_{hyd} / k_f \qquad (1)$$

where, the local heat transfer coefficient is obtained as follows:

$$h_z = q''_z / (T_{wm} - T_{fm}) \text{, and,} \qquad (2)$$

$$q''_z = -k_s (\partial T / \partial y)_z \qquad (3)$$

For all subsequent data processing, unless otherwise stated, we use the following two definitions for the wall and fluid temperatures respectively.

- For experimental data reduction

T_{wm} = local mean temperature of front surface of the channel wall, as measured by the IR camera

T_{fm} = linearly interpolated value between the fluid inlet and outlet temperatures at channel cross-

section corresponding to the two thermocouples locations T_{in} and T_{out} (Figure 1a).

Although, in the case of experiments, thermocouples could have been inserted in the flow to measure the fluid temperature, we observed that by doing so the velocity boundary layer was getting disturbed and the assumption of hydrodynamically fully developed flow was getting compromised. In fact, the local Nusselt number was coming to be higher than the predictions for hydrodynamically fully developed but thermally developing flows. Therefore, to capture the Nusselt number as close as possible, explicitly in the thermal development region only, we decided not to disturb the flow by inserting thermocouples in the channels. As will be seen later, although this makes the measurements non-intrusive, capturing the non-linear increase of fluid temperature in the channel, under the situations when axial back-conduction dominates, is then not recordable. Thus, the assumption of a linear temperature rise of the fluid as it passes through the channel is only valid so far as the conjugate effects are negligible. These aspects will be discussed subsequently. Local heat flux along the channel, q''_z in Eq. 3, is calculated from the IR thermograms; the local gradient of temperature and the k_s being known and assuming essentially a 1D conduction at the interface.

- For numerical data reduction

T_{wm} = peripheral averaged wall temperature at location of interest along the channel

T_{fm} = area averaged fluid temperature at the fluid cross-section of interest along the channel. In simulations, local fluid temperature is known.

Figure 2 shows the axial variation of local Nusselt number, Nu_z and thermograms of the front side of the fin exposed to IR camera, for two Reynolds numbers, respectively. The experimental results are plotted with their corresponding numerical simulations and it can be seen that agreement in results is reasonably good. For flow Re = 850, the channel length corresponds to z*= 0.006, a case of very early thermal boundary layer development. The wall temperature gradients are clearly visible, a unique advantage of IRT. Even at Re = 330, the flow is not thermally fully developed. The nature of the thermograms at any location in the streamwise direction, close to the fluid-solid boundary, suggests that the temperature gradient measured in the Y-direction, and thus the resulting heat flux, continuously varies. This is due to the axial flow of heat flux in the upstream direction due to the conjugate nature of the problem. Next, we scrutinize the effect of axial conduction in the substrate on the estimation of Nu_z. The constant heat flux applied at a distance from the fluid-solid interface has indeed got distorted, as we have seen in the thermograms in Fig 2. The pertinent question is: to what extent this distortion will affect the estimation of local Nusselt number? Figure 3(a) shows the simulation of local Nusselt number for two cases (i) Aluminum substrate, as used in the experiments, where $k_{sf} = (k_s/k_f) = 300$ and, (ii) A stainless steel substrate, where $k_{sf} = 26.6$. The simulated heat flux ratio for these two cases and the experimental data for aluminum substrate are also depicted. It is evident from this figure that the constant heat flux applied at a distance from the substrate no longer remains constant at the fluid-solid interface.

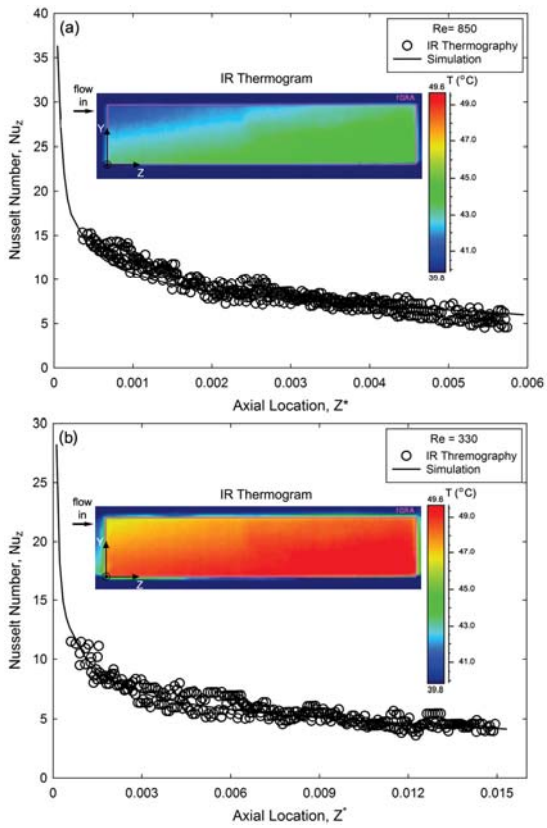

Figure 2: Axial variation of local Nusselt number at (a) Re = 850 and (b) Re = 330. Inset shown the actual IR thermograms

Figure 3(b) shows the corresponding wall and fluid temperatures for these two cases. The experimentally obtained wall temperature profile is also shown. As a reference case, the temperature profile for the UHF condition applied at the fluid solid interface is also drawn. Due to axial conduction in the substrate, there is a tendency of isothermalization of the wall temperature with increasing k_{sf}. In addition, as the heat flux does not remain constant at the fluid-solid interface, as noted earlier, the increase of fluid temperature becomes non-linear. It is rather difficult to experimentally capture this non-linearity of the fluid temperature without disturbing the velocity boundary layers.

Looking at the axial variation of Nusselt number and comparing it with the case of UHF (in Fig. 3(a)), we note that it is not affected drastically due to the change in the boundary condition, except at high Reynolds number and very early in the thermal development zone. This is due to the fact that, although the heat flux does not remain constant at the interface, the temperature difference between the wall and the fluid also changes in a way that Nu_z is only mildly affected.

SUMMARY AND CONCLUSIONS

Thermo-hydrodynamics of thermally developing single-phase flow of water through a square mini-channel has been experimentally carried out in the laminar region. The main conclusions are:

a) Developing flows provide very high heat transfer coefficients in the entrance regions and therefore of interest for mini/micro scale high heat flux removal applications.
b) IRT thermography can be successfully employed to experimentally determine Nu_z during the early thermal development region. Experimental Nu_z shows reasonable agreement with computations.
c) Nusselt numbers for UHF and the conjugate problems were numerically compared and it was shown that the deviation is not very high.
d) Higher value of k_{sf} leads to the isothermalization of interface wall temperature whereas a lower k_{sf} approaches to constant heat flux condition.

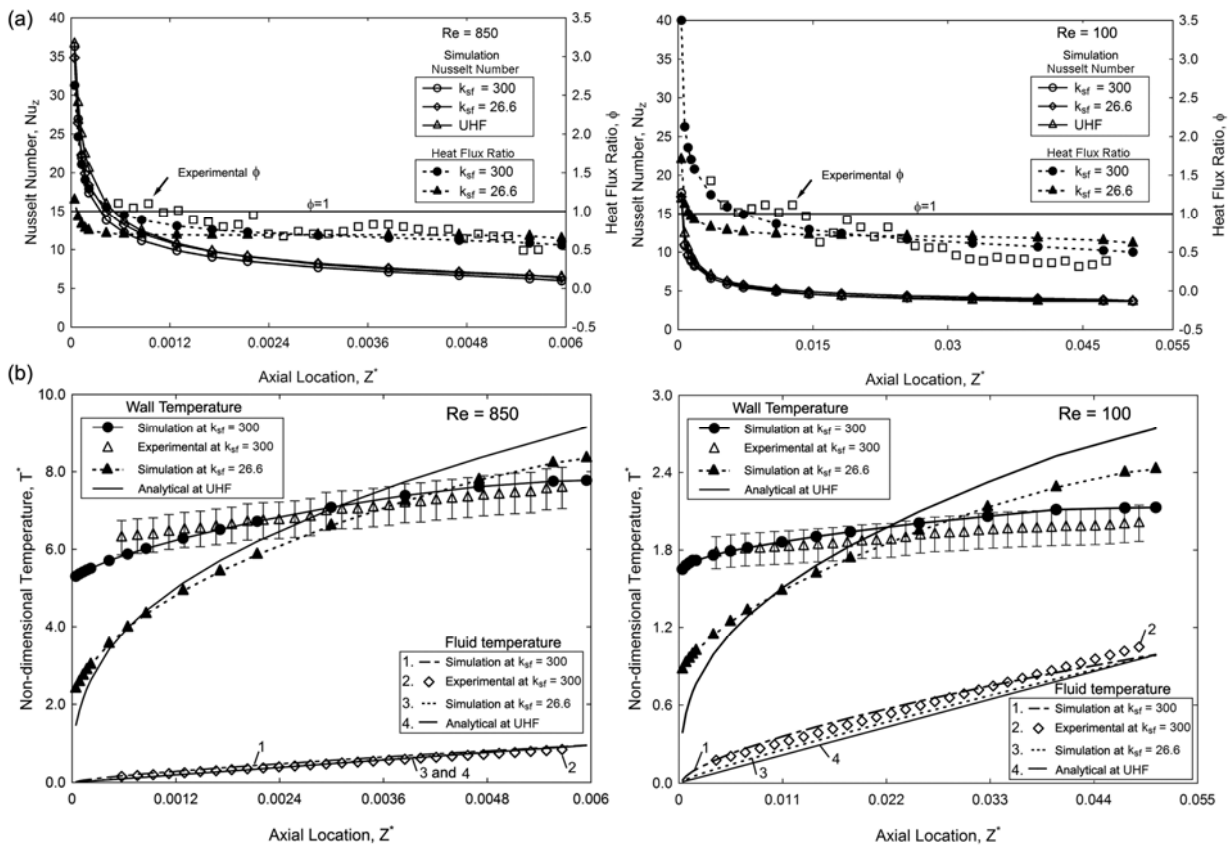

Figure 3: (a) Axial variation of local heat flux ratio and Nu_z for different values of k_{sf} and flow Re (b) Axial variation of non-dimensional wall and fluid temperature for different values of k_{sf} and flow Re.

NOMENCLATURE

A	area of cross section (m^2)
D_{hyd}	hydraulic diameter (m)
h	heat transfer coefficient (W/m^2K)
k	thermal conductivity (W/mK)
q''	heat flux (W/m^2)
T	temperature (K)
T^*	non-dimensional temperature (-)
u,v,w	velocity components (m/s)
X,Y,Z	Axes in Cartesian coordinates (m)
Z	distance from inlet (m)
Z^*	non-dimensional distance (= $Z/Re \cdot Pr \cdot D_h$)
Greek symbols	
φ	heat flux ratio $= q''_{sf} / q''_{app}$
δ	thickness of substrate
Non-dimensional Numbers	
Bi	Biot number $(h \cdot \delta / k_s)$
Nu	Nusselt Number $(h \cdot D_{hyd} / k_f)$
Pr	Prandtl Number $(\mu_f \cdot c_p / k_f)$
Re	Reynolds Number $(\rho_f \cdot u \cdot D_{hyd} / \mu_f)$
Subscripts	
app	applied
f	fluid domain
hyd	hydrodynamic
m	mean
s	Solid domain
s-f	solid-fluid interface
z	local value along Z axis

ACKNOWLEDGEMENTS

Financial grants from (i) Department of Science and Technology (IRHPA/FIST funding) and (ii) Indo-French Center for Promotion of Advanced Research are gratefully acknowledged.

REFERENCES

Astarita T., Cardone G., Carlomagno G. M., Meola C., A survey on infrared thermography for convective heat transfer measurements, Opt. Laser Technol. 32 (2000) 593-610.

Celata G.P., Cumo M., Maconi V., McPhail S. J., Zummo G., Microtube liquid single phase heat transfer in laminar flow, Int. J. Heat Mass Transf. 49(2006) 3538-3546.

Gamrat G., Favre-Marinet M., Asendrych D., Conduction and entrance effects on laminar liquid flow and heat transfer in rectangular microchannels, Int. J. Heat Mass Transf. 48(2005) 2943-2954.

Hetsroni G., Gurevich M., Mosyak A., Rozenblit R., Surface temperature measurements of a heated capillary by means of an infrared technique, Meas. Sci. Technol. 14 (2003) 807-814.

Hetsroni G., Mosyak A., Pogrebnyak E., Rozenblit R., Infrared temperature measurements in micro-channels and micro-fluid systems, Int. J. Thermal Sci. 50 (2011) 853-868.

Kakuta N., Kondo K., Ozaki A., Arimoto Y., Yamada Y., Temperature imaging of sub-millimeter-thick water using near infrared camera, Int. J. Heat Mass Transf. 52 (2009) 4221-4228.

Lee P. S., Garimella S. V., Thermally developing flow and heat transfer in rectangular microchannels of different aspect ratios, Int. J. Heat Mass Transf. 49 (2006) 3060-3067.

Lelea D., The conjugate heat transfer of the partially heated microchannels, Heat Mass Transf. 44 (2007) 33-41.

Luikov A. V., Conjugate convective heat transfer problems, Int. J. Heat Mass Transf. 17 (1974) 257-265.

Maranzana G., Perry I., Maillet D., Mini- and micro-channels: influence of axial conduction in the walls, Int. J. Heat Mass Tran. 47 (2004) 3993-4004.

Moharana M. K., Agarwal G. and Khandekar S., Axial Conduction in Single-phase Simultaneously Developing Flow in a Rectangular Mini-channel Array, Int. J. Thermal Sciences, 50 (2011) 1001-1012.

Nonino C., Savino S., Giudice-Del S., Mansutti L., Conjugate forced convection and the heat conduction in circular microchannels, Int. J. Heat Fluid Flow. 30 (2009) 823-830.

Rao M., Khandekar S., Simultaneously developing flows under conjugated conditions in a mini-channel array: Liquid crystal thermography and computational simulations, Heat Transf. Eng. 30 (2009) 751-761.

Sargent S. R., Hedlund C. R., Ligrani P. M., An infrared thermography imaging system for convective heat transfer measurements in complex flows, Meas. Sci. Technol. 9 (1998) 1974-1981.

Wang X., Peng X.F., Experimental investigation of liquid forced-convection heat transfer through micro-channel, Int. J. Heat Mass Tran. 37 (1994) 73-82.

Zhang S. X., He Y. L., Lauriat G., Tao W. Q., Numerical studies of simultaneously developing laminar flow and heat transfer in microtubes with thick wall and constant outside wall temperature, Int. J. Heat Mass Transf. 53 (2010) 3977-3989.